

Platinum(II) metal complexes as potential anti-*Trypanosoma cruzi* agents

Marisol Vieites^a, Lucía Otero^a, Diego Santos^a, Jeannette Toloza^b,
Roberto Figueroa^b, Ester Norambuena^c, Claudio Olea-Azar^b, Gabriela Aguirre^d,
Hugo Cerecetto^d, Mercedes González^d, Antonio Morello^e, Juan Diego Maya^e,
Beatriz Garat^f, Dinorah Gambino^{a,*}

^a Cátedra de Química Inorgánica, Facultad de Química, Universidad de la República, Gral. Flores 2124, C.C. 1157, 11800 Montevideo, Uruguay

^b Departamento de Química Inorgánica y Analítica, Facultad de Ciencias Químicas y Farmacéuticas, Universidad de Chile, Casilla 233, Santiago, Chile

^c Departamento de Química, Universidad Metropolitana de Ciencias de la Educación, Santiago, Chile

^d Laboratorio de Química Orgánica, Facultad de Química, Facultad de Ciencias, Universidad de la República, Iguá 4225, 11400 Montevideo, Uruguay

^e Programa de Farmacología Molecular y Clínica, ICBM, Facultad de Medicina, Universidad de Chile, Independencia 1027, Santiago, Chile

^f Laboratorio de Interacciones Moleculares, Facultad de Ciencias, Universidad de la República, Iguá 4225, 11400 Montevideo, Uruguay

Abstract

In the search for new therapeutic tools against Chagas' disease (American Trypanosomiasis) two series of new platinum(II) complexes with bioactive 5-nitrofuryl containing thiosemicarbazones as ligands were synthesized, characterized and *in vitro* evaluated. Most of the complexes showed IC₅₀ values in the μ M range against two different strains of *Trypanosoma cruzi*, causative agent of the disease, being as active as the anti-trypanosomal drug Nifurtimox. In particular, the coordination of L3 (4-ethyl-1-(5-nitrofurfurylidene)thiosemicarbazide) to Pt(II) forming [Pt(L3)₂] lead to almost a five-fold activity increase in respect to the free ligand. Trying to get an insight into the trypanocidal mechanism of action of these compounds, DNA and redox metabolism (intra-parasite free radical production) were evaluated as potential parasite targets. Results suggest that the complexes could inhibit parasite growth through a dual mechanism of action involving production of toxic free radicals by bioreduction and DNA interaction.

Keywords: Chagas' disease; Platinum; 5-Nitrofuryl containing thiosemicarbazones; Free radical production; N,S ligands

1. Introduction

According to WHO, infectious and parasitic diseases are major causes of human disease worldwide [1,2]. Although representing a tremendous burden when compared to other communicable diseases that receive a high level of attention

from health systems, a group of parasitic and infectious diseases, called neglected diseases, has been characterized by historically low investment by the pharmaceutical industry. Often, most affected populations are also the poorest and the most vulnerable and they are found mainly in tropical and subtropical areas of the world. Among these neglected diseases, Chagas' disease (American Trypanosomiasis) is the largest parasitic disease burden in the American continent, affecting approximately 20 million people from southern United States to southern Argentina. The morbidity and mortality associated with this disease in America are more than one order of magnitude higher than those caused by malaria, schistosomiasis or leishmaniasis

* Corresponding author. Tel.: +5982 9249739; fax: +5982 9241906.
E-mail address: dgambino@fq.edu.uy (D. Gambino).

[1,3]. The disease, caused by the flagellate protozoan parasite *Trypanosoma cruzi*, is mainly transmitted to humans in two ways, either by blood-sucking reduviid insects of *Triatominae* family which deposit their infective faeces on the skin of the host at the time of biting, or directly by transfusion of infected blood. Humans and a large number of species of domestic and wild animals constitute the reservoir of the parasite.

Despite the progress achieved in the study of *T. cruzi*'s biochemistry and physiology, in which several crucial enzymes for parasite survival, absent in the host, have been identified as potential new drug targets, the chemotherapy of this parasitic infection remains undeveloped and non effective method of immune prophylaxis is available. The treatment has been based on old and quite unspecific nitroaromatic drugs that have significant activity only in the acute phase of the disease and, when associated with long term treatments, give rise to severe side effects [4,5,6–8].

In the search for a pharmacological control of Chagas' disease, metal complexes appear to be a promising new approach [5,9–12]. In this sense, the design of complexes combining ligands bearing anti-trypanosomal activity and pharmacologically active metals has been successfully developed. This strategy takes advantage of the medicinal chemistry emerging drug discovery paradigm of developing agents that could modulate multiple targets simultaneously with the aim of enhancing efficacy or improving safety relative to drugs that address only a single target [13]. This current approach, based on the development of a single chemical entity as a dual inhibitor capable to modulate multiple targets simultaneously, has the advantage of lower risk of drug-drug interactions compared to cocktails or multicomponent drugs [13,14]. In the case of the metal complexation approach, the obtained metal compounds could act through dual or even multiple mechanisms of action by combining the pharmacological properties of both, the ligand and the metal, or at least lead to an additive effect [11,12]. The development of single agents that provide maximal anti-protozoal activity by acting against multiple parasitic targets could diminish host toxic effects by lowering therapeutic dose and/or circumvent the development of drug resistance [15]. Leading work performed by Sánchez-Delgado et al. drove to metal complexes of clotrimazole and ketoconazole intended for anti-trypanosome therapy. Synergistic effects were observed in most of the cases [11,12]. We have also been successfully working on the development of potential anti-trypanosome agents through this approach. A series of vanadyl bioactive compounds of aromatic amine *N*-oxides has been developed and exhaustively studied [16]. The anti-*T. cruzi* activity of two novel series of palladium compounds of bioactive 5-nitrofuryl containing thiosemicarbazones has been evaluated *in vitro* and some aspects related to their possible synergistic effect and dual or even multiple mechanisms of action have been investigated. These ligands had shown higher *in vitro* activity against *T. cruzi* than Nifurtimox, the

nitrofuranyl drug used in the past. Their main mode of action, as for other nitroheterocyclic antiparasitic agents, could be related to the intracellular reduction of the nitro moiety followed by redox cycling, yielding reactive oxygen species (ROS) known to cause cellular damage [17]. Results strongly suggested that the palladium complexes retained the mechanism of action of the thiosemicarbazone ligands, relying their trypanocidal action mainly on the production of oxidative stress as a result of their bioreduction to toxic free radicals and extensive redox cycling. Moreover, the complexes strongly interacted with DNA and were found to be irreversible inhibitors of trypanothione reductase, a parasite-specific enzyme with an essential role in the defense of trypanosomatids against oxidative stress [18]. Having these results in mind, platinum(II) coordination of this last series of bioactive ligands seemed interesting because of the postulated metabolic similarities between tumor cells and *T. cruzi*'s [11]. Platinum compounds have proven their effect on tumor cells and their ability to bind DNA as main anti-tumoral mechanism of action [19–21]. In addition, some Pt compounds have shown anti-*T. cruzi* activity acting through different mechanisms, like DNA interaction and irreversible inhibition of *T. cruzi*'s trypanothione reductase [5,22–24].

Based on this approach, in this work eight new platinum(II) complexes of the bioactive thiosemicarbazones shown in Fig. 1 have been synthesized and characterized. Two different compounds of the formula $[\text{PtCl}_2(\text{HL})]$ and $[\text{Pt}(\text{L})_2]$ were obtained for each ligand. Compounds were studied by elemental analyses, conductometry, electrospray ionization mass spectrometry (ESI-MS) and vibrational (IR and Raman) and ^1H NMR spectroscopies. Due to its potential relevance in determining biological activity through generation of toxic free radicals by intra-parasite bioreduction, electrochemical behavior was investigated by cyclic voltammetry. In addition, the electrochemical free radicals production was studied by electronic spin resonance technique (ESR). The *in vitro* anti-*T. cruzi* activity of most of the compounds has been stated against two different strains of the parasite. Furthermore, to get an insight into the probable mechanism of anti-trypanosomal action, the capacity to produce free radicals that could lead to parasite death was evaluated by ESR experiments in the parasite and by respiration measurements. In addition, compounds were tested for their DNA interaction ability. Results were compared with those previously reported for the free ligands and the analogous palladium(II) compounds [18].

2. Experimental

2.1. Materials

All common laboratory chemicals were purchased from commercial sources and used without further purification. $\text{K}_2[\text{PtCl}_4]$ was commercially available. All

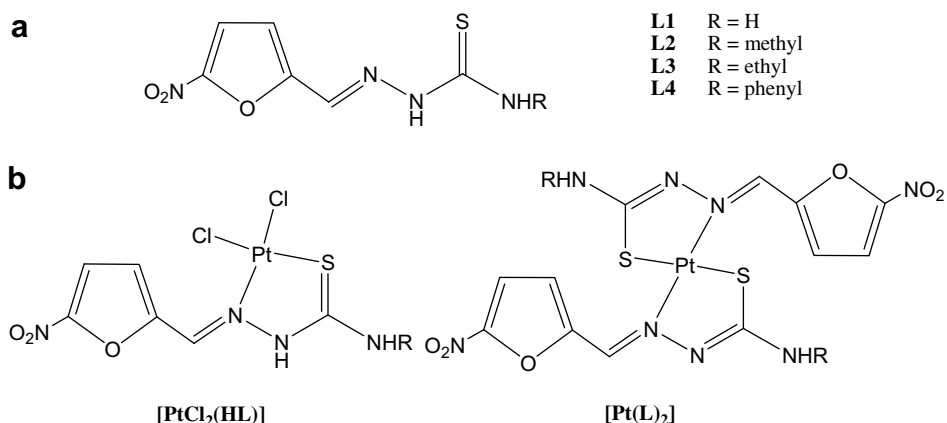


Fig. 1. Scheme showing: (a) the 5-nitrofuryl containing thiosemicarbazones selected as ligands and (b) the two series of platinum(II) complexes.

thiosemicarbazone ligands were synthesized using the previously reported technique [17].

2.2. Syntheses of the complexes

2.2.1. [PtCl₂(HL)] complexes, L: L1-L4

K₂[PtCl₄] (50 mg, 0.120 mmol) and the corresponding ligand (0.120 mmol) were heated under reflux in methanol (10 mL) during 6 h, after which a solid precipitated.

2.2.2. [Pt(L)₂] complexes, L: L1-L4

K₂[PtCl₄] (50 mg, 0.120 mmol) and the corresponding ligand (0.240 mmol) were heated under reflux in methanol (10 mL) during 6 h, after which a solid precipitated.

In all cases the obtained solid was filtered off and washed with hot methanol followed by warm water. Compounds were recrystallized by slow diffusion of water into a dimethylformamide (DMF) solution of each compound.

[PtCl₂(HL1)]. Brown solid, yield: 30 mg, 52%. Anal. calc. for C₆H₆Cl₂N₄O₃SPt: C, 15.01; H, 1.26; N, 11.67; S, 6.68. Found: C, 15.18; H, 1.25; N, 11.70; S, 6.67. ESI-MS (DMSO) *m/z*: 478.96 (M⁻), 442.98 (M-H-Cl)⁻, 408.98 (M-2Cl)⁻.

[PtCl₂(HL2)]. Red-brown solid, yield: 32 mg, 54%. Anal. calc. for C₇H₈Cl₂N₄O₃SPt: C, 17.01; H, 1.64; N, 11.34; S, 6.49. Found: C, 16.81; H, 1.67; N, 11.22; S, 6.35. ESI-MS (DMSO) *m/z*: 491.99 (M-H⁻), 457.01 (M-H-Cl)⁻.

[PtCl₂(HL3)]. Brown solid, yield: 27 mg, 44%. Anal. calc. for C₈H₁₀Cl₂N₄O₃SPt: C, 18.90; H, 1.98; N, 11.02; S, 6.30. Found: C, 19.02; H, 2.02; N, 11.24; S, 6.42.

[PtCl₂(HL4)]. Red-orange solid, yield: 28 mg, 42%. Anal. calc. for C₁₂H₁₀Cl₂N₄O₃SPt: C, 25.91; H, 1.81; N, 10.07; S, 5.76. Found: C, 26.01; H, 1.80; N, 10.29; S, 5.82.

[Pt(L1)₂]. Dark brown solid, yield: 39 mg, 52%. Anal. calc. for C₁₂H₁₀N₈O₆S₂Pt: C, 23.19; H, 1.62; N, 18.03; S, 10.31. Found: C, 23.08; H, 1.68; N, 18.01; S, 10.08. ESI-MS (DMSO) *m/z*: 621.96 (M+H)⁺, 620.07 (M-H)⁻.

[Pt(L2)₂]. Brown solid, yield: 28 mg, 36%. Anal. calc. for C₁₄H₁₄N₈O₆S₂Pt: C, 25.88; H, 2.17; N, 17.25; S, 9.87. Found: C, 25.79; H, 2.13; N, 16.93; S, 9.65.

[Pt(L3)₂]. Red-orange solid, yield: 48 mg, 78%. Anal. calc. for C₁₆H₁₈N₈O₆S₂Pt: C, 28.36; H, 2.67; N, 16.53; S, 9.46. Found: C, 28.06; H, 2.60; N, 16.39; S, 9.29.

[Pt(L4)₂]. Red-orange solid, yield: 43 mg, 46%. Anal. calc. For C₂₄H₁₈N₈O₆S₂Pt: C, 37.26; H, 2.34; N, 14.48; S, 8.28. Found: C, 36.83; H, 2.35; N, 14.28; S, 8.24.

2.3. Physicochemical characterization

C, H, N and S analyses were performed with a Carlo Erba Model EA1108 elemental analyzer. Conductimetric measurements were performed at 25 °C in 10⁻³ M DMF solutions using a Conductivity Meter 4310 Jenway [25]. Electrospray ionization mass spectra (ESI-MS) of dimethyl sulfoxide (DMSO) solutions of the complexes were recorded on a TSQ Thermo Finnigan equipment with a HESI probe at the analytical services of the Instituto Venezolano de Investigaciones Científicas (Caracas, Venezuela) and the quoted *m/z* values are for the major peaks in the isotope distribution. FTIR spectra (4000–400 cm⁻¹) of the complexes and the free ligand were measured as KBr pellets with a Bomen FTIR model MB102 instrument. Raman spectra were scanned with the FRA 106 accessory of a Bruker IF 66 FTIR spectrophotometer. The 1064 nm radiation of a Nd:YAG laser was used for excitation and 50–60 scans were routinely accumulated. ¹H NMR spectra of the complexes were recorded on a Bruker DPX-400 instrument at 400 MHz. Experiments were performed at 30 °C in acetone-*d*₆. Tetramethylsilane was used as the internal standard. Cyclic voltammetry (CV) was carried out on ca. 1.0 × 10⁻³ M DMSO (spectroscopic grade) solutions using a Metrohm 693 VA instrument with a 694 VA Stand convertor and a 693 VA Processor and a three-electrode cell under nitrogen atmosphere at room temperature with tetrabutyl ammonium perchlorate (TBA) (ca. 0.1 M) as supporting electrolyte. A hanging drop mercury electrode (HDME) was used as the working electrode, a platinum wire as the auxiliary electrode, and saturated calomel (SCE) as the reference electrode. ESR spectra of the free radicals obtained by electrolytic reduction were recorded

in the X band (9.85 GHz) using a Bruker ECS 106 spectrometer with a rectangular cavity and 50 kHz field modulation. Radicals of the Pt complexes were generated by electrolytic reduction *in situ* in 10^{-3} M DMSO solutions at room temperature under nitrogen atmosphere and the conditions previously established by cyclic voltammetry. Simulations of the ESR spectra were made using the software WINEPR Simphonia 1.25 version. The hyper-fine splitting constants were estimated to be accurate within 0.05 G [26].

2.4. *In vitro anti-T. cruzi activity*

Compounds were tested against epimastigote form of two strains of *T. cruzi*, namely Tulahuen 2 and Dm28c. Handling of live *T. cruzi* was done according to established guidelines [27].

2.4.1. Tulahuen 2 strain epimastigotes

The epimastigote form of the parasite Tulahuen 2 strain was grown at 28 °C in an axenic medium (BHI-tryptose), complemented with 5% fetal calf serum. Cells from a 5 days-old culture were inoculated into 50 mL of fresh culture medium to give an initial concentration of 1×10^6 cells/mL. Cell growth was followed by daily measuring the absorbance *A* of the culture at 600 nm for 11 days. Before inoculation, the media was supplemented with 10 μM or 25 μM of compounds from a stock DMSO solution. The final DMSO concentration in the culture media never exceeded 0.4% (vol/vol) and had no effect by itself on the proliferation of the parasites (no effect on epimastigote growth was observed by the presence of up to 1% DMSO in the culture media). The compounds ability to inhibit growth of the parasite was evaluated, in triplicate, in comparison to the control (no drug added to the media). The control was run in the presence of 0.4% DMSO and in the absence of any drug. The percentage of growth inhibition (PGI) was calculated as follows: $\% = \{1 - [(A_p - A_{0p}) / (A_c - A_{0c})]\} \times 100$, where $A_p = A_{600}$ of the culture containing the drug at day 5; $A_{0p} = A_{600}$ of the culture containing the drug just after addition of the inocula (day 0); $A_c = A_{600}$ of the culture in the absence of any drug (control) at day 5; $A_{0c} = A_{600}$ in the absence of the drug at day 0. Nifurtimox and Benznidazol were used as the reference trypanocidal drugs. After stating activity at the studied doses, dose-response curves were recorded and the IC₅₀ (50% inhibitory concentration) values were assessed [18]. Reported values are mean of three independent experiments.

2.4.2. Dm28c strain epimastigotes

T. cruzi epimastigotes Dm28c strain, from our own collection (Programa de Farmacología Molecular y Clínica, Facultad de Medicina, Universidad de Chile) were grown at 28 °C in Diamond's monophasic medium, as reported earlier [28] but replacing blood by 4 μM hemin. Fetal calf serum was added to a final concentration of 4%. Com-

pounds dissolved in DMSO (1% final concentration) were added to a suspension of 3×10^6 epimastigotes/mL. Parasite growth was followed by nephelometry for 10 days. No toxic effect of DMSO alone was observed at the final concentration. From the epimastigote exponential growth curve, the culture growth constant (*kc*) for each compound concentration treatment and for controls were calculated (regression coefficient >0.9 , $P < 0.05$). This constant corresponds to the slope resulting from plotting the natural logarithm (Ln) of nephelometry lecture versus time [29]. IC₅₀*kc* is the drug concentration needed to reduce the *kc* in 50% and it was calculated by lineal regression analysis from the *kc* values and the concentrations used at the employed concentrations. Reported values are mean of at least three independent experiments.

2.5. Calf thymus DNA interaction experiments

Complexes were tested for their DNA interaction ability using native calf thymus DNA (CT DNA) (Type I) by a modification of a previously reported procedure [18,30]. CT DNA (50 mg) was dissolved in water (30 mL) (overnight). Solutions of the complexes in DMSO (spectroscopy grade) (1 mL, 10^{-3} M) were incubated at 37 °C with solution of CT DNA (1 mL) during 96 h. DNA/complexes mixtures were exhaustively washed to eliminate the unreacted complex. Quantification of bound metal was done by atomic absorption spectroscopy on a Perkin Elmer 5000 spectrometer. Standards were prepared by diluting a metal standard solution for atomic absorption spectroscopy. Final DNA concentration per nucleotide was determined by UV absorption spectroscopy using molar absorption coefficient of $6000 \text{ M}^{-1} \text{ cm}^{-1}$ at 260 nm.

2.6. Free radicals production in *T. cruzi* (Dm28c strain)

The free radical production capacity of the new complexes was assessed in the parasite by ESR using 5,5-dimethyl-1-pyrroline-*N*-oxide (DMPO) for spin trapping. Each tested compound was dissolved in DMF (spectroscopy grade) (ca. 1 mM) and the solution was added to a mixture containing the epimastigote form of *T. cruzi* (Dm28c strain, final protein concentration 4–8 mg/mL) and DMPO (final concentration 250 mM). The mixture was transferred to a 50 μL capillary. ESR spectra were recorded in the X band (9.85 GHz) using a Bruker ECS 106 spectrometer with a rectangular cavity and 50 KHz field modulation. All the spectra were registered in the same scale after 15 scans [17].

2.7. Oxygen uptake

Dm28c strain *T. cruzi* epimastigotes were harvested by $500 \times g$ centrifugation, followed by washing and re-suspension in 0.05 M sodium phosphate buffer, pH 7.4, and containing 0.107 M sodium chloride. Respiration measurements were carried out polarographically with a Clark

electrode (Yellow Springs Instruments, 53 YSI model) [18,31]. An amount of parasites equivalent to 1.0 mg of protein/mL was added to a 0.6 mL chamber and oxygen consumption was recorded at 28 °C. Control respiration rate corresponded to 28 natoms gram of oxygen/min/mg protein. In order to evaluate redox cycling, mitochondrial respiration was inhibited with 2 mM potassium cyanide. For comparative purposes and in order to maintain a similar parasite to drug mass ratio in growth inhibition and in oxygen uptake experiments, metal compounds were used in a 1.25 mM final concentration in the oxygraph chamber. Results were corrected according to the observed effect produced by DMSO alone.

3. Results and discussion

Two new series of platinum(II) complexes, [PtCl₂(HL)] and [Pt(L)₂], with bioactive 5-nitrofuryl containing thiosemicarbazones (L) as ligands have been synthesized with high purities and good yields. All of them are neutral non conducting compounds and analytical and ESI mass spectrometry results are in agreement with the proposed formula. As shown below, N,S bidentate coordination was observed in all cases, remaining the ligand non deprotonated at the NH group for the [PtCl₂(HL)] compounds and deprotonated for the [Pt(L)₂] compounds.

3.1. IR and Raman spectroscopic studies

Based on experimental spectra and DFT studies, we have previously defined a characteristic vibrational (IR and Raman) spectroscopic pattern for 5-nitrofuryl thiosemicarbazones and their Pd(II) complexes, that allowed

us to analyze the spectroscopic behavior of the eight new Pt(II) complexes holding the 5-nitrofuran thiosemicarbazone moiety. IR and Raman spectra of the latter were compared with those previously reported for the free ligands and their Pd(II) analogues and main bands were tentatively assigned (Table 1) [32].

Although thiosemicarbazone ligands are potentially capable of interacting with metal centers in different ways, they usually coordinate to metals as N,S bidentate ligands. There are at least three major stretching vibrations that present strong diagnostic value in relation to the binding mode of these ligands: $\nu(\text{C}=\text{N})$, $\nu(\text{C}=\text{S})$ and $\nu(\text{N}-\text{N})$. As previously reported, for the selected 5-nitrofuryl containing thiosemicarbazones these bands are located in spectral regions showing a complicated signals pattern, that has made their assignment difficult [32]. In particular, thiosemicarbazone C=N and C=S stretchings are located in wave number regions where vibrations of other portions of the ligands occur, namely $\nu_{\text{as}}(\text{NO}_2)$ and 2-substituted furans out of-phase $\nu(\text{C}=\text{C})$, occurring in the C=N stretching region (1650–1500 cm⁻¹), and $\delta(\text{NO}_2)$, furan scissoring vibrations and furan hydrogen wagging symmetric modes and combination of them, occurring in the C=S stretching region (850–700 cm⁻¹). The combination of experimental and DFT theoretical methods had previously allowed us to explain the complexity of the observed spectral pattern of these ligands and their Pd(II) complexes and to perform an assignment of the C=N and N–N stretchings. Although clear changes were observed in the spectral region around 750–900 cm⁻¹, the C=S stretching, that is usually used as probe of the coordination of the metal to the thiocarbonyl sulfur, could not be undoubtedly assigned for the palladium complexes due to the high complexity of the spectra [32].

Table 1
Tentative assignment of the main characteristic IR and Raman bands of the platinum complexes

Compound	IR/cm ⁻¹						Raman/cm ⁻¹			
	$\nu(\text{C}=\text{N})$	$\nu_{\text{s}}(\text{NO}_2)$	$\nu(\text{C}-\text{O}-\text{C}) + \text{C}-\text{C}$ contract ^a	$\nu(\text{N}-\text{N})^{\text{b}}$	$\nu(\text{C}-\text{S})^{\text{c}}$	$\delta(\text{NO}_2) + \text{furan}^{\text{d}}$	$\nu(\text{C}=\text{N})$	$\nu(\text{C}=\text{C})^{\text{e}}$	$\nu_{\text{s}}(\text{NO}_2)$	$\nu(\text{C}-\text{O}-\text{C}) + \text{C}-\text{C}$ contract ^a
L1	1602 s	1356 s	na	1108	846	811	1592 m	1455 s	1351 m	1339 m
[PtCl ₂ (HL1)]	1570 vw	1347 s	na	1170		812	1568 m	1454 s	1354 w	na
[Pt(L1) ₂]	1557 w	1352 s	1335 s	1157		812	1563 s	1450 s	1348 m	1329 m
L2	1599 w	1354 s	na	1114	820	808	1585 br	1474 s	1347 s	1312 m
PtCl ₂ (HL2)	1560 s	1349 s	na	1173		812	1554 sh	1470 s	na	1335 s
[Pt(L2) ₂]	1579 w	1350 s	1338 m	1169		811	1580 s	1469 s	1343 sh	1332 m
L3	1602 w	1352 s	na	1104	823	805	1601 m	1470 s	1351 s	1331 m
[PtCl ₂ (HL3)]	1590 w	1344 s	na	1175		811	1594 m	1470 s	1355 sh	1324 m
[Pt(L3) ₂]	1577 w	1350 s	1333 s	1156		810	1575 s	1471 s	1349 m	1330 s
L4	1595 m	1344 s	na	1104	822	811	1596 m	1474 s	1346 m	1321 m
[PtCl ₂ (HL4)]	1600 m	1347 s	na	1175		811	1599 s	1466 s	1340 s	1319 sh
[Pt(L4) ₂]	1584 vw	1353 s	1339 sh	1084		812	1578 s	1472 s	1333 s	1312 sh

ν : stretching; δ : bending; s: strong, m: medium; w: weak.

na: non assigned.

Bands previously reported for the free ligands are included for comparison [32].

^a Furan C–O–C in-phase stretching + C–C contract.

^b Medium.

^c Weak to very weak.

^d $\delta(\text{NO}_2)$ + furan modes or furan hydrogen wagging symmetric modes.

^e Furan in-phase C=C stretching.

The vibrational spectra of the newly developed platinum complexes showed a very similar pattern to that of the corresponding palladium complexes. Although the complexity of the IR spectra of the ligands and, concomitantly of their metal complexes, increased from L1 to L4 as the R-substituent complexity increased, a common spectral pattern could be observed for each series of platinum compounds ($[\text{PtCl}_2(\text{HL})]$ and $[\text{Pt}(\text{L})_2]$). As shown in Table 1, after coordination $\nu(\text{C}=\text{N})$ bands of the free thiosemicarbazone ligands shifted in almost all cases to lower wave numbers. This modification is consistent with coordination of the thiosemicarbazone ligands through the azomethine nitrogen. On the other hand, the shift to higher wave numbers of the $\nu(\text{N}-\text{N})$ band, observed for the platinum complexes, has also been previously related to the electronic delocalization produced as a consequence of coordination through the azomethine nitrogen atom and/or deprotonation of the thiosemicarbazone ligands [32]. The $\nu(\text{C}=\text{S})$ bands should shift to lower wave numbers when thiosemicarbazones coordinate through the thiocarbonyl sulfur. For the Pt complexes weak to very weak sets of bands were detected in the $700\text{--}850\text{ cm}^{-1}$ region, some of them probably associated with $\nu(\text{CS})$ vibrations. As it was the case for the Pd analogues, the complexity of the spectra in this region due to vibrations assigned to the nitrofuran moiety and mixing of vibrations superimposed to a very significant intensity decrease of the $\text{C}=\text{S}$ bands experimentally observed after coordination of thiosemicarbazones to a metal made the unambiguous assignment of the $\text{C}=\text{S}$ bands difficult. Nevertheless, clear changes observed in this spectral region agree with the coordination of the thiocarbonyl sulfur to platinum [32]. In agreement with the reported formulae of the complexes, the $\nu(\text{NH})$ band, at approximately $3120\text{--}3150\text{ cm}^{-1}$, is present in all $[\text{PtCl}_2(\text{HL})]$ complexes indicating that the ligand is non deprotonated in these neutral complexes. In contrast, $\nu(\text{NH})$ band is not observed in all $[\text{Pt}(\text{L})_2]$ complexes due to deprotonation of the ligands. Taking into account the crystal structure of $[\text{Pd}(\text{L}5)_2] \cdot 3\text{DMSO}$ previously reported [18] and the great similarities in vibrational spectral pattern shown by the Pd and Pt analogous compounds, a *trans* configuration is proposed for the $[\text{Pt}(\text{L})_2]$ complexes (Fig. 1). Calculations previously performed for the $[\text{Pd}(\text{L})_2]$ complexes are also in agreement with this proposal [32]. Vibrations associated to those portions of the ligands that are not involved in the coordination to the metal were also recognized in the spectra of the complexes and are also shown in Table 1: nitro moiety symmetric stretching ($\nu_s(\text{NO}_2)$), furan combination mode involving furan $\text{C}-\text{O}-\text{C}$ in-phase stretching and $\text{C}-\text{C}$ contract ($\nu(\text{C}-\text{O}-\text{C}) + \text{C}-\text{C}$ contract) and $\delta(\text{NO}_2) + \text{furan}$ modes or furan hydrogen wagging symmetric modes.

3.2. NMR studies

The complexes were characterized by ^1H NMR spectroscopy. The low solubility of many of the complexes did not allow to acquire the complete series of ^1H NMR

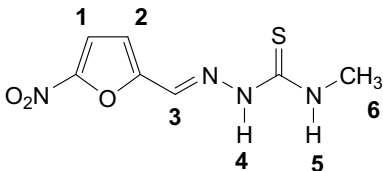
spectra. Platinum complexes and their palladium analogues showed similar NMR spectra and behavior [18]. Results of the performed NMR experiments are in agreement with the proposed structures and with the results of the other spectroscopies. ^1H NMR integrations and signal multiplicities are in agreement with the proposed formula. As an example results for $\text{PtCl}_2(\text{HL}2)$ are shown in Table 2. ^1H NMR chemical shifts (δ) of the ligand and the complex, and the chemical shift differences between complex and ligand, expressed as $\Delta\delta$, are shown. The attached figure shows the numbering scheme of the free ligand mentioned in the Table and the text. Pt and Pd complexes showed similar ^1H chemical shifts of the nitrofurylthiosemicarbazone common portion of their molecules [18]. When the ligand is coordinated, the effect of the metal is apparent for the protons that are located close to the coordinating atoms, the azomethine nitrogen (H3 according to Table 2) and the NH exchangeable protons (H4 and H5, see Table 2). The presence of a signal corresponding to proton H4 is in accordance with the coordination of the ligand in a non deprotonated form. Furthermore, the largest $\Delta\delta$ are observed for this proton.

3.3. Cyclic voltammetry

Voltammetric studies were mainly performed to determine the effect of platinum complexation on the peak potential of the nitro moiety due to the biological significance of this potential in relation to the capability of the compounds to be bioreduced in the parasite leading to the toxic nitro anion radical species.

Fig. 2 shows, as examples, the cyclic voltammograms for $[\text{PtCl}_2(\text{HL}3)]$ and $[\text{Pt}(\text{L}3)_2]$ at 2000 mV/s (a) and for $[\text{PtCl}_2(\text{HL}3)]$ when scan rate is changed in the range $100\text{--}2000\text{ mV/s}$ (b). All Pt complexes displayed comparable voltammetric behavior, showing three well-defined reduction waves in DMSO as shown by the free ligands [18,26].

Table 2
 ^1H NMR chemical shift values (δ) in ppm of L2 [18] and $[\text{PtCl}_2(\text{HL}2)]$ at $30\text{ }^\circ\text{C}$



^1H NMR	L2		$\Delta\delta^a$
	δ_{Ligand}^b	$\delta_{\text{Complex}}^c$	
H			
1	7.79	7.67	-0.12
2	7.30	7.54	0.24
3	7.98	7.84	-0.14
4	11.87	8.90	-2.97
5	8.52	8.40	-0.14
6	3.03	3.10	0.07

^a $\Delta\delta = (\delta_{\text{Complex}} - \delta_{\text{Ligand}})$.

^b $\text{DMSO-}d_6$.

^c $\text{Acetone-}d_6$.

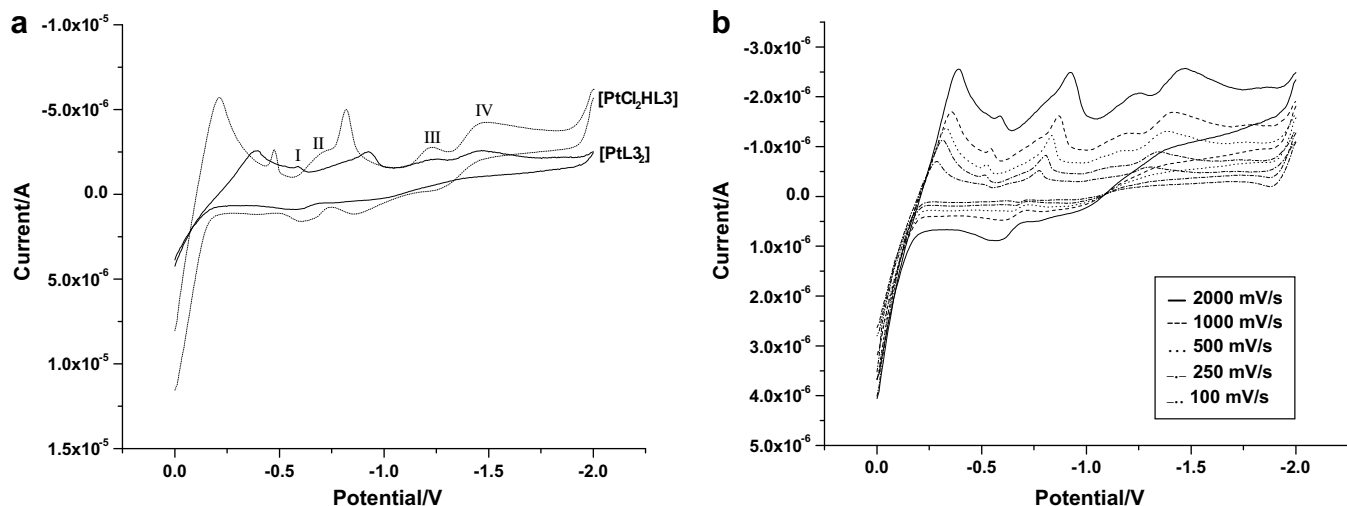


Fig. 2. Cyclic voltammograms of 1 mM DMSO solutions, 0.1 M TBAP, of: (a) $[\text{PtCl}_2(\text{HL}3)]$ and $[\text{Pt}(\text{L}3)_2]$ at 2000 mV/s and (b) $[\text{PtCl}_2(\text{HL}3)]$ when scan rate is changed in the range 100–2000 mV/s.

The first wave for all the Pt compounds corresponded to a quasireversible process involving a one-electron transfer (couple II). This wave around -0.80 V versus SCE corresponds to the generation of the anion radical RNO_2^- by reduction of the nitro group [18,33]. The reverse scan showed the anodic counterpart of the reduction wave. According to the standard reversibility criteria this couple can be attributed to a diffusion-controlled one-electron transfer. For some complexes, sharp peaks around this couple could be observed as a result of adsorption phenomena in the electrode surface due to the presence in the molecules of the thiocarbonyl group and the metal. This phenomenon has been also observed for the Pd analogues [33]. Next two couples (III and IV) are assigned to the reduction of the platinum complex nitro anion radical generated in the first couple. Subsequent less negative three-electron irreversible cathodic peak (IIIc, Fig. 2a) is irreversible in the whole range of sweep rates used (100–2000 mV/s) and can be attributed to the production of the hydroxylamine derivative [26,34]. Peak IVc is presumed to belong to the reduction of the imine moiety ($\text{CH}=\text{N}$) of the thiosemicarbazone group [35].

Small differences were found between $[\text{PtCl}_2(\text{HL})]$ and $[\text{Pt}(\text{L})_2]$ complexes, as previously observed for the Pd analogous compounds [33]. The voltammogram of $[\text{PdCl}_2\text{HL}]$ complexes showed a prepeak (Ic, Fig. 2a) that appeared even before the reduction of the nitro group, meaning that the nitro group follows another reaction path besides the known electron-transfer mechanism of the nitroaromatic compounds in aprotic media. This prepeak would correspond to the four-electron reduction of a small portion of the molecules reaching the electrode surface, while the remaining portion would supply the protons required for this reduction. This is a typical behavior of a self-protonation phenomenon displayed by nitrocompounds with acidic moieties in their structures [26,33,34]. The presence of the nitro group

increases the acidity of the NH moiety of the thiosemicarbazone group present only in the $[\text{PtCl}_2(\text{HL})]$ complexes (L non deprotonated) which becomes capable of protonating the nitro group of a minor part of the molecules in the solution, resulting into a lower intensity of these signals. $[\text{Pt}(\text{L})_2]$ complexes did not show the Ic prepeak because they do not have the capability to protonate the nitro group since the NH proton was lost as a consequence of coordination of the ligand to platinum.

Table 3 lists the values of voltammetric peaks for all studied compounds. The potentials of the voltammetric peaks corresponding to the nitro moiety of the free ligands slightly changed as a consequence of platinum complexation, being the latter only slightly more favourable than the former and than those previously reported for the palladium analogues [18,26]. However, it should be stated that all studied compounds showed under the same conditions a higher capacity to be reduced than Nifurtimox ($E_{1/2}$

Table 3

Cyclic voltammetric parameters for the reduction of the platinum complexes corresponding to the couple II, peak Ic, IIIc and IVc measured in DMSO at 2000 mV/s

Compound	$E_{\text{pIc}}^{\text{a}}$	$E_{\text{pIIIc}}^{\text{a}}$	$E_{\text{pIIa}}^{\text{b}}$	$E_{\text{pIIIc}}^{\text{a}}$	$E_{\text{pIVc}}^{\text{a}}$
$[\text{PtCl}_2(\text{HL}1)]$	-0.43	-0.70	-0.66	-1.209	-1.51
$[\text{Pt}(\text{L}1)_2]$	–	-0.69	-0.56	-1.22	-1.49
$[\text{PtCl}_2(\text{HL}2)]$	-0.49	-0.73	-0.60	-1.17	-1.37
$[\text{Pt}(\text{L}2)_2]$	–	-0.68	-0.70	-1.34	-1.65
$[\text{PtCl}_2(\text{HL}3)]$	-0.58	-0.84	-0.58	-1.25	-1.46
$[\text{Pt}(\text{L}3)_2]$	–	-0.77	-0.61	-1.22	-1.49
$[\text{PtCl}_2(\text{HL}4)]$	na	-0.78	-0.56	-1.17	-1.37
$[\text{Pt}(\text{L}4)_2]$	–	-0.72	-0.62	-1.09	-1.26
Nfx [18]		-0.91	-0.85		

Nfx: Nifurtimox; na: not assigned.

Potentials are reported in volts versus saturated calomel electrode.

^a E_{pc} : cathodic peak potential.

^b E_{pa} : anodic peak potential.

−0.88 V, Table 3) and therefore a better ability to generate radical species that could be toxic for the parasite [36].

3.4. Free radicals production studied by ESR spectroscopy

The complexes were tested for their capability to produce free radicals in reductive conditions. The free radicals characterized by ESR were prepared “*in situ*” by electrochemical reduction in DMSO, applying a potential corresponding to the first monoelectronic wave (IIc/IIa) obtained from the cyclic voltammetric experiments. The interpretation of the ESR spectra by means of a simulation process has led to the determination of the hyperfine coupling constants for all the magnetic nuclei. The obtained hyperfine constants are listed in Table 4.

The ESR spectra of the [PtCl₂(HL)] complexes were simulated in terms of one triplet corresponding to the nitrogen nucleus belonging to the nitro group and one triplet to the nitrogen of the C=N thiosemicarbazone group and three doublets due to non-equivalent hydrogens belonging to the side chain. Other nuclei presented hyperfine constant smaller than the line width.

The ESR spectra of the [Pt(L)₂] complexes were analyzed in terms of one triplet due to the nitrogen of the nitro group, two doublets due to hydrogens corresponding to the furan ring and one triplet due to hydrogens, having very similar hyperfine constants, belonging to the thiosemicarbazone chains. Other hyperfine constants resulted smaller than the line width and they were not observed in the experimental spectrum. Fig. 3 shows the ESR spectrum of complex [Pt(L₂)₂].

Different substituents in the thiosemicarbazone chain of the coordinated ligands did not seem to affect the hyperfine pattern of platinum complexes as it had been previously observed for the corresponding palladium ones. However, the number of ligands coordinated per Pt central atom seemed to determine spin density distribution and so the hyperfine pattern of the complexes. For the [Pt(L)₂] complexes, the spin density was more located on the nitro furan ring while other observed couplings could be related to non completely equivalent thiosemicarbazone ligands coordinated to the platinum atom. For the [PtCl₂(HL)] com-

Table 4
Hyperfine splittings (gauss) for the anion radical of the platinum complexes

	aN	aN	aH	aH	aH	aH	aH
[PtCl ₂ (HL1)]	6.95	4.1	1.28	1.4	1.12	<0.6	<0.6
[Pt(L1) ₂]	6.8	<0.6	0.8	4.0	<0.6	2.45	2.35
[PtCl ₂ (HL2)]	6.97	3.5	1.2	1.5	1.00	<0.6	<0.6
[Pt(L2) ₂]	7.0	<0.6	1.2	4.0	<0.6	3.1	3.3
[PtCl ₂ (HL3)]	6.90	3.7	1.15	1.6	1.28	<0.6	<0.6
[Pt(L3) ₂]	7.0	<0.6	1.24	4.0	<0.6	3.0	3.3
[PtCl ₂ (HL4)]	6.87	4.0	1.17	1.25	1.3	<0.6	<0.6
[Pt(L4) ₂]	7.2	<0.6	1.10	3.8	<0.6	2.98	3.10

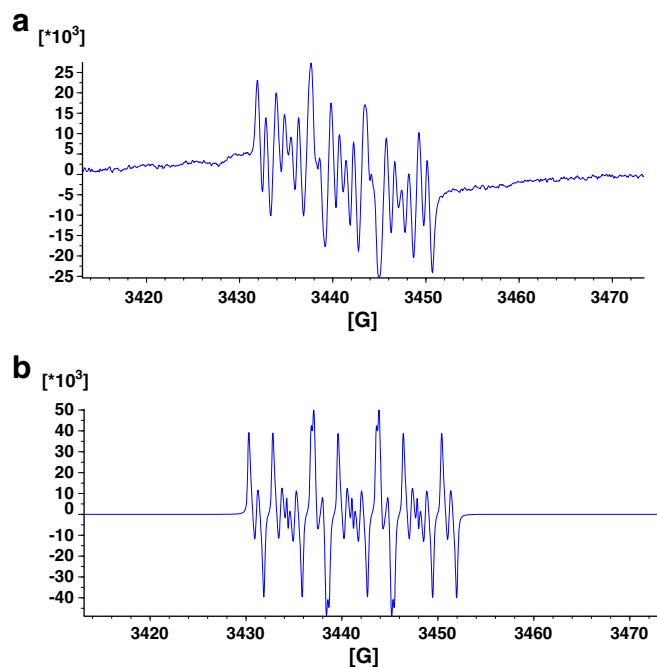


Fig. 3. (a) ESR experimental spectrum of [Pt(L₂)₂]. Spectrometer conditions: microwave frequency 9.71 GHz; microwave power 20 mW; modulation amplitude 0.2 G; scan rate 1.25 G/s; time constant 0.5 s; number of scans 15. (b) Simulated spectrum of [Pt(L₂)₂].

pounds, the spin density was more delocalized on the entire radical.

The effect of changing the metal atom on the hyperfine pattern of the ESR spectra of the complexes should be noted. For palladium complexes, no differences have been observed between [PdCl₂(HL)] and [Pd(L)₂] ones. Both series of palladium compounds presented a quite similar hyperfine pattern to that observed for the [PtCl₂(HL)] complexes. The different observed ESR pattern for [M(L)₂] complexes when changing palladium by platinum could be related to small differences in complexes structure. This fact would also agree with a quite different biological behavior.

3.5. *In vitro* anti *T. cruzi* activity

The existence of the epimastigote form of *T. cruzi* as an obligate mammalian intracellular stage has been confirmed recently [37,38]. Therefore, compounds were tested *in vitro* against epimastigote form of the parasite. The complexes were evaluated for their anti-*T. cruzi* activities against epimastigotes of Tulahuen 2 strain in order to compare with previously performed biological evaluation of the free ligands and the analogous Pd complexes. Fifty percent of inhibitory concentrations (IC₅₀) obtained from dose – response curves are depicted in Table 5. In addition, some complexes were evaluated against a second strain of *T. cruzi* epimastigotes, namely Dm28c.

For comparative purposes Table 5 also includes IC₅₀ values for the four free ligands and the Pd complexes,

Table 5
In vitro biological activity of the Pt complexes

Compound	<i>T. cruzi</i> (Tulahuen 2) PGI ^a		IC ₅₀ ^b	<i>T. cruzi</i> (Dm28c) IC ₅₀ ^b	Compound	<i>T. cruzi</i> (Tulahuen 2) IC ₅₀ ^c
	10 μM	25 μM				
[PtCl ₂ (HL1)]	10.9	38.2	>25	nd	L1	2.7
[Pt(L1) ₂]	3.4	20.8	>25	nd	[PdCl ₂ (HL1)]	2.4
					[Pd(L1) ₂]	4.5
					L2	5.0
[PtCl ₂ (HL2)]	41.5	60.5	13.1	36.7	[PdCl ₂ (HL2)]	4.3
[Pt(L2) ₂]	68.4	100	6.9	10.2	[Pd(L2) ₂]	4.7
					L3	4.9
[PtCl ₂ (HL3)]	26.9	44.1	27.5	nd	[PdCl ₂ (HL3)]	5.9
[Pt(L3) ₂]	100	100	0.8	28.8	[Pd(L3) ₂]	>25
					L4	>25
[PtCl ₂ (HL4)]	33.8	72.0	15	28.4	[PdCl ₂ (HL4)]	>25
[Pt(L4) ₂]	18.9	12.1	>25	41.3	[Pd(L4) ₂]	>25
Benznidazol			7.4	38.0		
Nifurtimox			6.1 [17]	22.8		

IC₅₀ values of the free ligand and their Pd complexes on *T. cruzi* (Tulahuen 2 strain) have been included for comparison [18].

nd: not determined.

^a PGI: percentage of growth inhibition of *T. cruzi* epimastigote cells at the specified dose.

^b ±10%.

^c [18].

previously determined through the same technique on epimastigote form of *T. cruzi* Tulahuen 2 strain [18]. Most of the Pt complexes were active against epimastigotes of *T. cruzi* Tulahuen 2 strain, showing some of them IC₅₀ values of the same order than Nifurtimox and the corresponding free ligands. According to the IC₅₀ values [Pt(L3)₂] and [Pt(L2)₂] were the most active Pt complexes against this parasite strain, being [Pt(L3)₂] significantly more active than L3 and than Nifurtimox.

When the results are compared with those previously reported for the free ligands and the Pd analogous compounds, it can be stated that the activity pattern is significantly modified by changing the central atom. The activity of the Pd complexes followed the general trend: [PdCl₂(HL)] > free ligand > [Pd(L)₂]. This regular trend was not observed for the Pt analogues. This different behavior could be related with differences in bioavailability, unspecific toxicity and/or mechanism of action of both series of metal complexes.

Similar general conclusions can be obtained from the analysis of the activity results on the *T. cruzi* Dm28c strain, although some strain susceptibility differences can be observed. Dm28c is a parasite clone that had previously shown to be less susceptible to Nifurtimox and Benznidazol trypanocidal effect than Tulahuen strain, which is mediated by a Dm28c higher thiol content of the former [39].

3.6. Capacity of derivatives to generate free radical species into *T. cruzi*

The complexes were incubated with intact *T. cruzi* (Dm28c strain) epimastigotes in the presence of DMPO

as spin trapping agent in order to detect possible intracellular free radical species produced by bioreduction and having short half-lives. The biological free radical production capacity of the new compounds was assessed by ESR. All the compounds were capable to produce free radicals in the intact parasite giving an ESR spectrum. Fig. 4 shows, as an example, the ESR spectrum obtained when [PtCl₂(HL2)] was incubated with *T. cruzi* in the presence of DMPO. The typical hyperfine pattern of adducts obtained when DMPO traps radicals centered in C atom

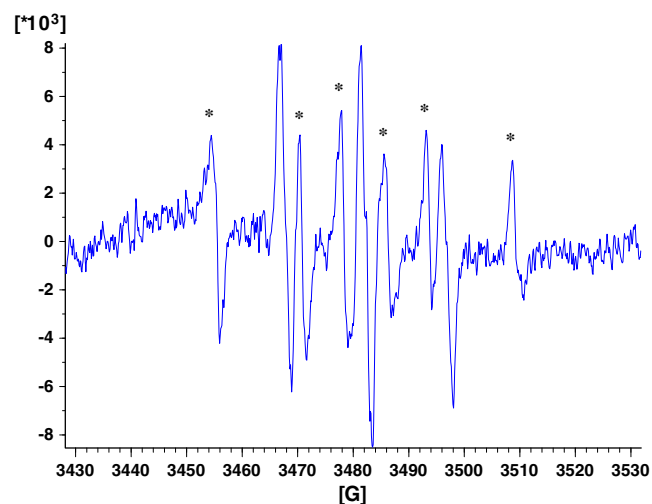


Fig. 4. ESR spectrum of [PtCl₂(HL2)] obtained when [PtCl₂(HL2)] was incubated with *T. cruzi* epimastigotes in the presence of DMPO. Spectrometer conditions: microwave frequency 9.68 GHz, microwave power 20 mW, modulation amplitude 0.2 G, scan rate 1.25 G/s, time constant 0.5 s, number of scans: 15. * signals of DMPO-nitro anion radical adduct.

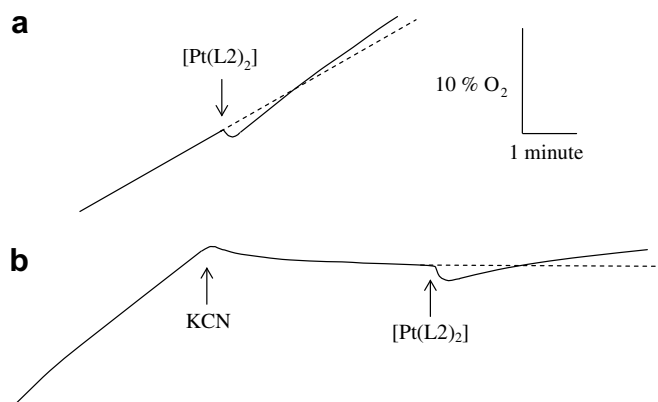


Fig. 5. (a) Effect of compound $[Pt(L)_2]$ on the parasite (*T. cruzi*, Dm28c strain) oxygen consumption related to control (dotted line). (b) Effect of compound $[Pt(L)_2]$ on the parasite (*T. cruzi*, Dm28c strain) oxygen consumption after inhibition of the respiration with KCN related to control (dotted line).

($aN = 16.7$ G and $aH = 22.5$ G) was observed [18]. A triplet produced by DMPO decomposition was also detected [40].

ESR studies showed that the newly developed Pt thiosemicarbazone complexes were bioreduced in the parasite, indicating that they could maintain the mode of action of the 5-nitrofuryl pharmacophore.

3.7. Oxygen uptake

The involvement of the platinum complexes in redox cycling processes should increase the parasite oxygen consumption. Thus, the effect of the compounds on parasite oxygen uptake was measured. The effect of complex $[Pt(L)_2]$ on *T. cruzi* epimastigotes oxygen consumption with and without inhibition of the respiration with KCN is shown in Fig. 5. Both series of complexes modified oxygen uptake by the parasite increasing oxygen consumption (Table 6). These results are in accordance with a bioreductive and redox cycling mechanism of action as previously reported for the free 5-nitrofuryl containing thiosemicarbazones, their Pd complexes and other nitrofurans derivatives like Nifurtimox [18,41]. For both series of compounds effect on parasite respiration seemed to correlate with the IC_{50} values. For instance, $[Pt(L)_3]$ being the most active Pt compound, showed the highest increase on oxygen consumption.

3.8. Calf thymus DNA interaction

In order to address if interaction with DNA could be part of the mode of action of the complexes, experiments with CT DNA were carried out. Binding of the Pt complexes to DNA was studied by combining atomic absorption determinations (for the metal) and electronic absorption measurements for DNA quantification. The new complexes are good binding agents for CT DNA

Table 6
Effect of the addition of Pt complexes on oxygen uptake by *T. cruzi* epimastigotes (Dm28c strain)

Compound	Respiration (nanoatom-gram of O/min/mg protein)	Increase on oxygen consumption (%) ^a
Control	28.0 ± 2.0	
$[PtCl_2(HL)_2]$	32.2 ± 3.2	15
$[Pt(L)_2]$	31.3 ± 1.7	12
$[Pt(L)_3]$	39.2 ± 4.2	40
$[PtCl_2(HL)_4]$	35.5 ± 3.2	27
$[Pt(L)_4]$	32.0 ± 1.3	14
Nifurtimox	35.6 ± 0.8	27

^a % increase on oxygen consumption after addition of 1.25 mM of compounds with respect to control (no added compound).

Table 7
Interaction of Pt complexes with CT DNA after 96 h of incubation at 37 °C

Compound	nmol Pt/mg DNA	Metal/base ^a	Base/metal
$[PtCl_2(HL)_1]$	209	0.069	14
$[Pt(L)_1]$	390	0.129	8
$[PtCl_2(HL)_2]$	236	0.078	13
$[Pt(L)_2]$	224	0.074	14
$[PtCl_2(HL)_3]$	191	0.063	16
$[Pt(L)_3]$	527	0.174	6
$[PtCl_2(HL)_4]$	170	0.056	18
$[Pt(L)_4]$	170	0.056	18

^a Platinum (mol) per DNA base (mol).

(Table 7). Although the determined platinum to DNA binding levels were similar to those of known anti-tumor metal complexes they resulted significantly lower than those of the palladium analogous compounds [18,19]. No general pattern could be detected for both series of compounds, being binding levels almost not affected by the nature of the thiosemicarbazone ligand. $[PtCl_2(HL)]$ complexes, having labile chloride ligands could probably interact with DNA through a mechanism similar to that previously reported for cisplatin, becoming activated through aquation and reacting with nucleophilic DNA bases [42]. $[Pt(L)_2]$ complexes cannot act in this way, but they could intercalate DNA or interact through other mechanisms. Due to the planar motive contained in the $[PtCl_2(HL)]$ complexes, intercalation could also be possible for these compounds. Further studies are under progress in order to get an insight into the mechanism of this interaction. It is interesting to note that $[Pt(L)_3]$, being the most potent anti-*T. cruzi* compound of the series showed the highest interaction with DNA. Nevertheless, $[Pt(L)_1]$ being almost non active strongly interacts with DNA, showing that the mechanism of trypanocidal activity could not involve only DNA as target.

4. Conclusions

Pt(II) complexes with 5-nitrofuryl containing thiosemicarbazones as bioactive ligands showed good anti-trypanosomal activity. In particular, the coordination of L3 to

Pt(II) forming [Pt(L3)₂] lead to almost a five-fold activity increase in respect to the free ligand. Possible targets, namely reductive metabolism (intra-parasite free radical production) and DNA, were screened trying to get insight into the mechanism of action of these metal compounds. Results showed that some of the compounds could act as dual inhibitors in the parasite, through production of toxic free radicals and interaction with DNA.

Results of this work show that the approach of coordinating anti-trypanosomal organic compounds with pharmacologically interesting metals could be a suitable strategy to develop novel therapeutic tools against tropical diseases produced by trypanosomatids, particularly American Trypanosomiasis.

Acknowledgments

This work was partially supported by PEDECIBA and Universidad de La República (CSIC project 364/06) of Uruguay, Prosul-CNPq project 490209/2005-0, SIBAS-0807 UMCE, FONDECYT Chile 1061072 and CONICYT-PBCT Anillo ACT 29. We wish to thank Dr. E.J. Baran, CEQUINOR, UNLP, Argentina for Raman spectra facilities and Matilde Gómez, Instituto Venezolano de Investigaciones Científicas, Caracas, Venezuela for performing ESI-MS experiments.

References

- [1] <http://www.who.int/>; <<http://www.who.int/ctd/chagas>>.
- [2] D. Engels, L. Savioli, *Trend Parasitol.* 22 (2006) 363–366.
- [3] J. Urbina, *Expert Opin. Ther. Pat.* 13 (2003) 661–669.
- [4] H. Cerecetto, M. González, *Curr. Topics Med. Chem.* 2 (2002) 1185–1190.
- [5] R.L. Krauth-Siegel, H. Bauer, R.H. Schirmer, *Angew. Chem. Int. Ed.* 44 (2005) 690–715.
- [6] S. Croft, M. Barret, J. Urbina, *Trend Parasitol.* 21 (2005) 508–512.
- [7] M. Ceaser, *The Lancet Infect. Dis.* 5 (8) (2005) 470–471.
- [8] Y. Yamagata, J. Nakagawa, *Adv. Parasitol.* 61 (2006) 129–165.
- [9] C. Zhang, S. Lippard, *Curr. Opin. Chem. Biol.* 7 (2003) 481–489.
- [10] N.P. Farrell, *Metal Complexes as Drugs and Chemotherapeutic Agents*, in: J.M. McCleverty, T.J. Meyer (Eds.), *Comprehensive Coordination Chemistry II*, vol. 9, Elsevier, 2003, pp. 809–840.
- [11] R.A. Sánchez-Delgado, A. Anzellotti, L. Suárez, *Metal complexes as chemotherapeutic agents against tropical diseases: malaria, trypanosomiasis, and leishmaniasis*, in: H. Sigel, A. Sigel (Eds.), *Metal Ions in Biological Systems*, vol. 41, Marcel Dekker, New York, 2004, pp. 379–419.
- [12] R.A. Sánchez-Delgado, A. Anzellotti, *Mini-Rev. Med. Chem.* 4 (2004) 23–30.
- [13] R. Morphy, Z. Rankovic, *J. Med. Chem.* 48 (2005) 6523–6543.
- [14] Z. Wang, E.M. Bennett, D.J. Wilson, C. Salomon, R. Vince, *J. Med. Chem.* 50 (2007) 3416–3419.
- [15] K. Chibale, *Towards broad spectrum antiprotozoal agents. ARKI-VOC IX*, 2002, pp. 93–98.
- [16] C. Urquiola, M. Vieites, G. Aguirre, A. Marín, B. Solano, G. Arrambide, M.L. Lavaggi, M.H. Torre, M. González, A. Monge, D. Gambino, H. Cerecetto, *Bioorg. Med. Chem.* 14 (2006) 5503–5509.
- [17] G. Aguirre, H. Cerecetto, M. González, D. Gambino, L. Otero, C. Olea-Azar, C. Rigol, A. Denicola, *Bioorg. Med. Chem.* 12 (2004) 4885–4893.
- [18] L. Otero, M. Vieites, L. Boiani, A. Denicola, C. Rigol, L. Opazo, C. Olea-Azar, J.D. Maya, A. Morello, R.L. Krauth-Siegel, O.E. Piro, E. Castellano, M. González, D. Gambino, H. Cerecetto, *J. Med. Chem.* 49 (2006) 3322–3331.
- [19] A. Gómez-Quiroga, C. Navarro-Ranninger, *Coord. Chem. Rev.* 248 (2004) 119–133.
- [20] M.D. Hall, T.W. Hambley, *Coord. Chem. Rev.* 232 (2002) 49–67.
- [21] T.W. Hambley, *Coord. Chem. Rev.* 166 (1997) 181–223.
- [22] S. Bonse, J.M. Richards, S.A. Ross, G. Lowe, R.L. Krauth-Siegel, *J. Med. Chem.* 43 (2000) 4812–4821.
- [23] G. Lowe, A.S. Droz, T. Vilaiyan, G.W. Weaver, L. Tweedale, J.M. Pratt, P. Rock, V. Yardley, S.L. Croft, *J. Med. Chem.* 42 (1999) 999–1006.
- [24] S.L. Croft, *Mem. Inst. Oswaldo Cruz* 94 (1999) 215–220.
- [25] W.J. Geary, *Coord. Chem. Rev.* 7 (1971) 81–91.
- [26] C. Rigol, C. Olea-Azar, F. Mendizábal, L. Otero, D. Gambino, M. González, H. Cerecetto, *Spectrochim. Acta A* 61 (2005) 2933–2938.
- [27] L. Huang, A. Lee, J.A. Ellman, *J. Med. Chem.* 45 (2002) 676–684.
- [28] J.D. Maya, A. Morello, Y. Repetto, R. Tellez, A. Rodríguez, U. Zelada, P. Puebla, M. Bontá, S. Bollo, A. San Feliciano, *Comp. Biochem. Phys. C* 125 (2000) 103–109.
- [29] M.A. Cuellar, C. Salas, M.J. Cortés, A. Morello, J.D. Maya, M.D. Preitea, *Bioorg. Med. Chem.* 11 (2003) 2489–2497.
- [30] R.E. Mahnken, M.A. Billadeau, E.P. Nikonowicz, H. Morrison, *J. Am. Chem. Soc.* 114 (1992) 9253–9265.
- [31] M.E. Letelier, E. Rodríguez, A. Wallace, M. Lorca, Y. Repetto, A. Morello, J. Aldunate, *Exp. Parasitol.* 71 (1990) 357–363.
- [32] D. Gambino, L. Otero, M. Vieites, M. Boiani, M. González, E.J. Baran, H. Cerecetto, *Spectrochim. Acta A* 68 (2007) 341–348.
- [33] L. Otero, C. Folch, G. Barriga, C. Rigol, L. Opazo, M. Vieites, D. Gambino, H. Cerecetto, E. Norambuena, C. Olea-Azar, *Spectrochim. Acta A*, <<http://dx.doi.org/10.1016/j.saa.2007.07.045>>.
- [34] C. Olea-Azar, C. Rigol, F. Mendizábal, A. Morello, J.D. Maya, C. Moncada, E. Cabrera, R. Di Maio, M. Gonzalez, H. Cerecetto, *Free Rad. Res.* 37 (2003) 993–1001.
- [35] S. Bollo, E. Soto-Bustamante, L.J. Núñez-Vergara, J.A. Squella, *J. Electroanal. Chem.* 492 (2000) 54–62.
- [36] C. Olea-Azar, A.M. Atria, F. Mendizábal, R. Di Maio, G. Seoane, H. Cerecetto, *Spectrosc. Lett.* 31 (1998) 99–109.
- [37] V.J. Arán, C. Ochoa, L. Boiani, P. Buccino, H. Cerecetto, A. Gerpe, M. González, D. Montero, J.J. Nogal, A. Gómez-Barrio, A. Azqueta, A. López de Ceraín, O.E. Piro, E.E. Castellano, *Bioorg. Med. Chem.* 13 (2005) 3197–3207.
- [38] K.M. Tyler, D.M. Engman, *Int. J. Parasitol.* 31 (2001) 472–480.
- [39] Y. Repetto, E. Opazo, J.D. Maya, M. Agosin, A. Morello, *Comp. Biochem. Phys. B* 115 (1996) 281–285.
- [40] N. Veerapen, S.A. Taylor, C.J. Walsby, B. Mario Pinto, *J. Am. Chem. Soc.* 128 (2006) 227–239.
- [41] J.D. Maya, S. Bollo, L.J. Núñez-Vergara, J.A. Squella, Y. Repetto, A. Morello, J. Périé, G. Chauvière, *Biochem. Pharmacol.* 65 (2003) 999–1006.
- [42] V. Brabec, *Prog. Nucl. Acid Res. Mol. Biol.* 71 (2002) 1–68.